*Journal of Information Display*
Vol. 13, No. 1, March 2012, 21–30

Taylor & Francis
Taylor & Francis Group

# A controller design for high-quality images on microcapsule active-matrix electrophoretic displays

Chi-Ming Lu[a,b*] and Chin-Long Wey[a]

[a]*Department of Electrical Engineering, National Central University, Jhongli 32001, Taiwan, Republic of China*
[b]*Small & Medium-Sized New-Technology Development, Chung-Hwa Picture Tubes, Ltd., Taoyuan 33409, Taiwan, Republic of China*

(*Received 5 September 2011; Revised 2 December 2011; Accepted for publication 5 December 2011*)

Active-matrix electrophoretic display (AMEPD) is commonly used for the applications of smart handheld reading devices such as e-books and e-news. This paper presents a new reduced waveform lookup table storage method that reduces the associated lookup table by approximately $2n$ ($n$ is the number of gray levels employed) times the conventional one. The paper also proposes a driving method for image display. The method provides high-speed performance for image display and also effectively eliminates the image residue, achieving high image quality. The prototyped controller was connected to a 6" AMEPD panel, whose excellent display quality demonstrated the effectiveness of the proposed controller design.

**Keywords:** active-matrix electrophoretic display; display controller; LUT; electronic readers; electronic papers

## 1. Introduction

Smart handheld reading devices such as e-readers or e-papers require low power supply, lightweight devices, and high-resolution display [1]. The electrophoretic display (EPD) is lightweight, thin, and flexible, has a wide viewing angle, and can be read in all lighting conditions. These, and the fact that it is bi-stable, invariably reflective, and has a paper-like quality, make the EPD ideal for application in smart handheld reading devices.

There are two types of EPD driving methods: the passive driving method and the active-matrix thin-film transistor (TFT) driving method. Owing to its salient features of high resolution and better display quality, the active-matrix EPD (AMEPD) technology is commonly adopted for portable handheld devices. Figure 1 shows a commercial microcapsule AMEPD and its backend system board. The basic functions of the display controller include the controls of the (1) panel resolution; (2) signal timing of the source/gate driver ICs for the TFT switches; and (3) magnitudes of the driving voltages [2].

The grayscale of the images in the microcapsule AMEPD technology is displayed by the differential driving voltages on the pixel electrodes with a fixed DC voltage on the common electrode. The pulse-width modulation is generally realized by applying the positive and negative voltage states in different scanning frames. Note that the voltage state transition for illustrating the grayscale is called the *driving waveform*. The display quality of driving waveforms for the display controller highly depends on the grayscale stability, display reliability, and image updating speed.

Owing to the nonlinearity of the electrical–optical response of the EPD film, it is virtually very difficult to determine the driving waveform from the device equations. It must thus be customized to satisfy the different specification demands of driving speed, bi-stability, and contrast ratio [3–5].

This paper presents an effective and efficient display controller design in the board level. It also provides a driving method for effectively eliminating the image residue and achieving high image quality. The next section briefly reviews the display device technologies. Section 3 presents the driving waveform generation and proposed driving method. The hardware design of the proposed controller and the experiment results are described in Section 4. Finally, concluding remarks are given in Section 5.

## 2. Display device background

Figure 2 illustrates the structure of microcapsule EPDs, where both white (positively charged) and black (negatively charged) particles move between two electrodes in the transparent liquid within a microcapsule. The image is displayed by the motion of the charged particles, and the motion is determined by the applied electric field. The particles stay at the desired state when an appropriate electric field across both the pixel electrodes and the common electrode is applied [6].

*Corresponding author. Email: littlerichs@yahoo.com.tw

ISSN 1598-0316 print/ISSN 2158-1606 online

http://dx.doi.org/10.1080/15980316.2011.650865
http://www.tandfonline.com

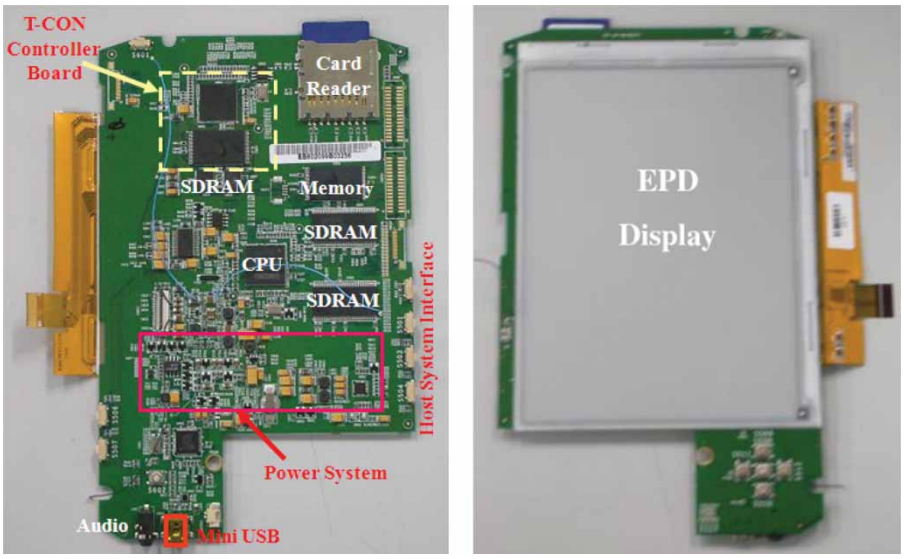


Figure 1. Commercial microcapsule AMEPD and its backend system board.

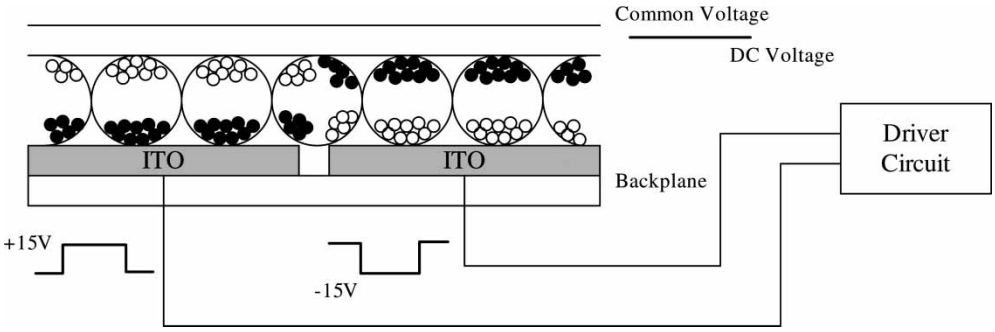


Figure 2. Typical microcapsule EPD.

### 2.1. *Gray-level determination*

The grayscale of the images in the microcapsule EPD technology is displayed by the differential driving voltage (generally, the positive or negative 15 V) on the pixel electrodes with a fixed DC voltage on the common electrode [7–9].

A positive pulse voltage drives the white particles to move upward while a negative pulse voltage causes the white particles to move downward [10]. The time duration of applying the pulse voltage determines the particle position and thus displays the desired gray level. Figure 3 describes the process of displaying the desired gray level.

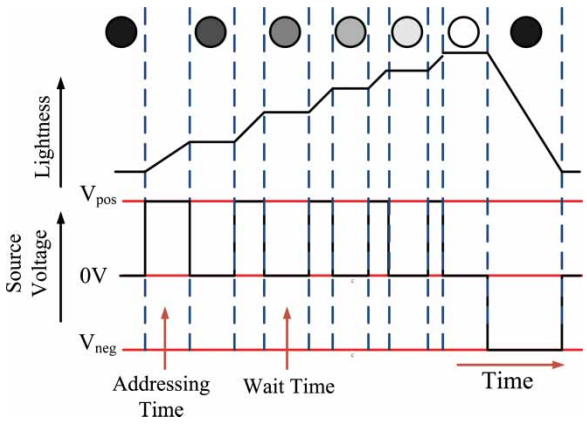


Figure 3. Determination of the gray levels in the microcapsule EPD.

### 2.2. *Driving method*

Directly driving panels with the driving waveform shown in Figure 3 may result in incorrect gray levels and may cause the residue image problem. Before a new image is displayed, the previous image must be efficiently and effectively erased. For high-quality applications, it is highly prohibited to display the residue of the previous image and the incorrect grayscales of the current image. The previous image can be completely erased through initialization and addressing, as shown in Figure 4.

As EPD particles are bi-stable, the displacement of such particles is based on the period of the driving voltage and can be stopped at the desired position when the zero voltage is supplied. It is not necessary to wait for the particles arriving at the target state. Therefore, the previous image

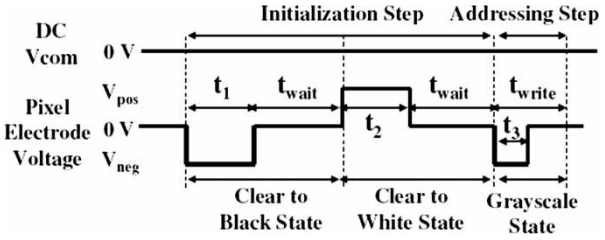


Figure 4. Traditional driving waveforms for the microcapsule EPD.

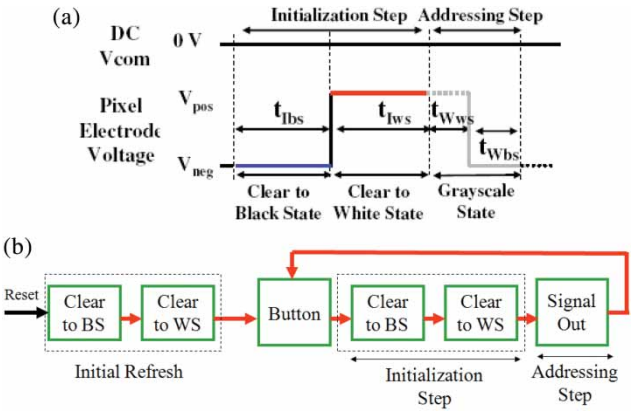


Figure 5. Driving method for the microcapsule EPD [11].

can be completely erased through initialization (I-step) and addressing (A-step), as shown in Figure 5(a) [11].

The EPD first clears to the black state (BS) and then the white state (WS) in I-step, then displays the grayscale state (GS) in A-step. Let $f_w$ be the number of frames for driving the EPD to the desired GS of the current image, and $f_{Iws}$ ($f_{Ibs}$) the number of frames for clearing the EPD to WS (BS) in I-step. The total number of frames required for updating an image is ($f_{Ibs} + f_{Iws} + f_w$).

In A-step, a gray level is defined and generated by first applying $f_{Wws}$ frames in WS and then $f_{Wbs}$ frames in BS, where $f_w = f_{Wws} + f_{Wbs}$. Owing to its bi-stability, the EPD will stay at WS unless a negative voltage ($V_{neg}$) is applied to it. Thus, displaying the first $f_{Wws}$ frames in WS in A-step is nothing, but just idle for $f_{Wws}$ frames because the EPD is already at WS. After the $f_{Wws}$ frame time, the $f_{Wbs}$ frames in BS are then displayed. Figure 5(b) illustrates the driving method, where an initial refresh procedure is applied before displaying the desired images. When the user presses the button for displaying a new image again, the controller reads the new image from the storage device and displays the new image via initialization and addressing.

### 2.3. *Lookup table size*

Let $k$ be the total number of scanning frames for changing the state of a pixel from a gray level to another gray level, and $f_w$ the number of frames required for driving to the desired grayscales of the current image. For a typical commercial display, the scanning frame rate is 60 Hz (i.e. 16.7 ms), and the response time for the state change (i.e. change from WS to BS or from BS to WS) ranges from 250 to 350 ms. Thus, the typical value of $f_w$ ranges from 15 to 21 frames. For the driving waveform in Figure 5(a), with $f_{Ibs} = f_{Iws} = f_w$, the total number of scanning frames for changing the state of a pixel from a gray level to another gray level is $k = 3 \times f_w$ (i.e. $k$ ranges from $15 \times 3$ (= 45) to $21 \times 3$ (= 63) frames).

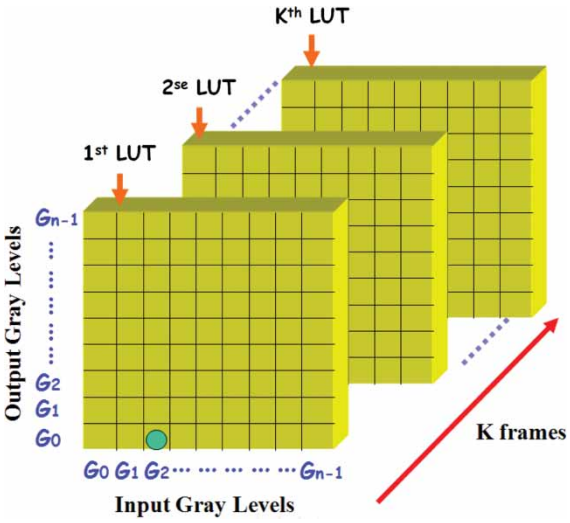


Figure 6. Traditional driving waveform lookup table.

With the conventional driving waveform lookup table, as shown in Figure 6, there are ($n^*n$) waveform entries that need to be edited, where $n$ is the maximum number of supported gray levels in a controller. Each entry in the table records a driving waveform to erase the previous gray level and then shows a new target gray level. This results in a total of ($n^*n^*k$) entries. For example, as shown by the green dot in Figure 6, the driving waveform that erases the G2 gray level of the previous images and then shows the G0 gray level of the current images during the period of $k$ frame time is stored.

As each entry contains a voltage state (+15, 0, or −15), two bits (01, 00, and 10) are required to represent the voltage state. Thus, the memory size for the conventional method is ($2^*n^*n^*k$) bits. For the typical displays with $n = 16$ gray levels and whose $k$ values range from 45 to 63 frames, the memory size ranges from 23 to 32 kbits.

## 3. Driving waveforms

This section presents the driving waveform generation and proposed driving method for high image quality.

### 3.1. *Driving waveform generation*

The measurement of the mono colors of the EPD film is generally conducted by using the GretagMacbeth Eye-One Pro spectrophotometer, as shown in Figure 7(a), where the

(a)

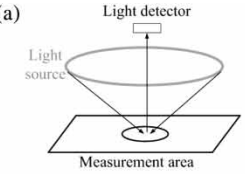


(b)

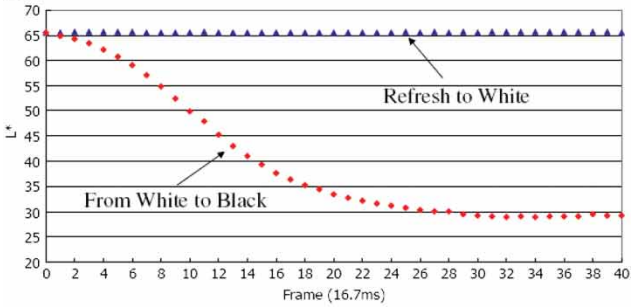


(c)

| Frame | Lightness | Frame | Lightness | Frame | Lightness | Frame | Lightness |
|---|---|---|---|---|---|---|---|
| 0 | 65.5721 | 10 | 49.9741 | 20 | 33.5460 | 30 | 29.3381 |
| 1 | 64.7868 | 11 | 47.9983 | 21 | 32.8267 | 31 | 29.1013 |
| 2 | 64.2831 | 12 | 45.2205 | 22 | 32.2133 | 32 | 29.0496 |
| 3 | 63.3436 | 13 | 43.0146 | 23 | 31.6223 | 33 | 29.0770 |
| 4 | 62.1058 | 14 | 41.0764 | 24 | 31.1769 | 34 | 29.0362 |
| 5 | 60.6671 | 15 | 39.3474 | 25 | 30.7532 | 35 | 29.0660 |
| 6 | 58.9906 | 16 | 37.7600 | 26 | 30.3810 | 36 | 29.0875 |
| 7 | 57.0306 | 17 | 36.4859 | 27 | 30.0949 | 37 | 29.1186 |
| 8 | 54.8867 | 18 | 35.3299 | 28 | 30.1643 | 38 | 29.5153 |
| 9 | 52.4743 | 19 | 34.4029 | 29 | 29.5736 | 39 | 29.2014 |
| | | | | | | 40 | 29.2849 |

(d)

| Frame | Lightness | Normalized | Gray | Frame | Lightness | Normalized | Gray |
|---|---|---|---|---|---|---|---|
| 0 | 65.5721 | 65.5721 | G15 | 10 | 49.9741 | 48.7721 | G5 |
| 1 | 64.7868 | 63.8921 | G14 | 11 | 47.9983 | 47.0921 | G4 |
| 2 | 64.2831 | 62.2121 | G13 | 12 | 45.2205 | 45.4121 | G3 |
| 3 | 63.3436 | 60.5321 | G12 | 13 | 43.0146 | 43.7321 | G2 |
| 4 | 62.1058 | 58.8521 | G11 | 14 | 41.0764 | 42.0521 | |
| 5 | 60.6671 | 57.1721 | G10 | 15 | 39.3474 | 40.3721 | G1 |
| 6 | 58.9906 | 55.4921 | G9 | 16 | 37.7600 | 38.6921 | |
| 7 | 57.0306 | 53.8121 | G8 | 17 | 36.4859 | 37.0121 | |
| 8 | 54.8867 | 52.1321 | G7 | 18 | 35.3299 | 35.3299 | G0 |
| 9 | 52.4743 | 50.4521 | G6 | | | | |

(e)

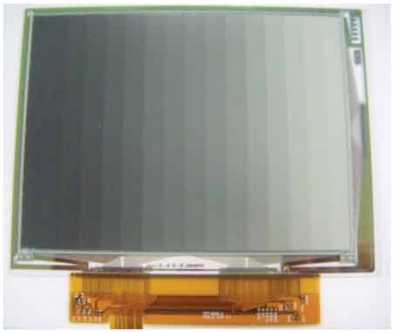

Figure 7. Gray-level definition: (a) spectrophotometer; (b) the measurement results; (c) the measured data; (d) the 16 gray levels through the straightforward approach; and (e) the 16 gray levels' picture.

ring light source is used. The measurement geometry and aperture are 45/0 and 4.5 mm, respectively. The measured data are lightness values in units of $L^*$ for a 2° observer under D65. Note that $L^*$ is a unit of lightness, as defined in the CIE 1976 standard. To simplify the discussion herein of the driving waveform generation, an EPD film will be taken as an example.

In this measurement, 40 frames of +15 V are first applied to drive the EPD to the WS. The resulting lightness $L^*$ is defined as frame 0 and the WS. Then, −15 V is applied to drive the EPD for one frame time (60 Hz, 16.7 ms), and lightness $L^*$ is defined as frame 1. The next step is to apply 40 frames of +15 V again to drive the EPD to the WS, then to apply −15 V to drive the EPD for two frame times (i.e. 33.5 ms). Lightness $L^*$ is defined as frame 2. This process is repeatedly applied to define the remaining frames.

Figure 7(b) plots the measurement results of the lightness for frames 0–40, where the actual measured data are tabulated in Figure 7(c). As the response time of this EPD film is approximately 292.9 ms, with the scanning frame rate 60 Hz of the EPD (i.e. 16.7 ms), the number of frames required to go from WS to BS can be estimated as 292.2/16.7 or 18 frames. The lightness at frame 0 is thus defined as a WS, and that at frame 18 as a BS. In this method, the minimum response time of the EPD with 16 grayscales is 16.7 ms × 16, or 267.2 ms. In other words, if the response time is faster, the proposed method still holds if the scanning frame rate of the EPD can be increased (e.g. 120 Hz).

It should be mentioned that the lightness of the defined WS (at frame 0) is virtually the same as that of the actual WS. As plotted in Figure 7(b), the maximal and minimal lightness of the WS are 65.65 and 65.54, respectively. On the other hand, the lightness of the defined WS at frame 0 in Figure 7(c) is approximately 65.58. This concludes that the defined WS is the actual WS, and that the WS is virtually invariant from frame 0 to 40. The salient feature of the stable WS is used herein for resolving the residual image, and for further improving the image quality.

This implementation proposes a straightforward approach to defining the 16 gray levels from frame 0 to 18, as tabulated at the 'normalized' column in Figure 7(d). The 16 gray levels are denoted as G$i$, $i = 0, 1, \ldots, 15$, and the lightness of a frame is labeled G$i$ if it is the closest to the available normalized value from G15 to G0. As shown in Figure 7(d), frames 0–13 are defined as G15–G2, respectively, while frames 15 and 18 are assigned to G1 and G0, respectively. Note that G1 was adjusted to frame 15 instead of 14 for better quality. Figure 7(e) shows the 16 aforementioned defined gray levels, and the EPD worked properly in the applications herein.

Table 1 shows the data regarding the gray-level definition. The table size is $(n^* f_w)$, where $n$ is the number of gray levels and $f_w$ is the number of frames for GS. With $n = 16$ and $f_w = 18$, the total size is 288 bits. For EPD displays, the conventional lookup table requires a size of $(2^* n^* n^* f_w)$, which is 9216 bits. The table reduction is $(2n)$ times, or 32 times.

Table 1 contains 18 × 16 entries, where each entry has only one bit. The total memory size for the lookup table is 288 bits. When the lookup table is used in I-step, both G0 and G15 are used for 'clear to BS' and 'clear to WS', respectively. States 0 and 1 imply $V_{pos}$ (= +15 V) and $V_{neg}$ (= −15 V), respectively. On the other hand, when

Table 1. Driving waveform lookup table.

| | Frames | | | | | | | | | | | | | | | | | |
|---|---|---|---|---|---|---|---|---|---|---|---|---|---|---|---|---|---|---|
| Gray | 1 | 2 | 3 | 4 | 5 | 6 | 7 | 8 | 9 | 10 | 11 | 12 | 13 | 14 | 15 | 16 | 17 | 18 |
| G15 | 0 | 0 | 0 | 0 | 0 | 0 | 0 | 0 | 0 | 0 | 0 | 0 | 0 | 0 | 0 | 0 | 0 | 0 |
| G14 | 0 | 0 | 0 | 0 | 0 | 0 | 0 | 0 | 0 | 0 | 0 | 0 | 0 | 0 | 0 | 0 | 0 | 1 |
| G13 | 0 | 0 | 0 | 0 | 0 | 0 | 0 | 0 | 0 | 0 | 0 | 0 | 0 | 0 | 0 | 0 | 1 | 1 |
| G12 | 0 | 0 | 0 | 0 | 0 | 0 | 0 | 0 | 0 | 0 | 0 | 0 | 0 | 0 | 0 | 1 | 1 | 1 |
| G11 | 0 | 0 | 0 | 0 | 0 | 0 | 0 | 0 | 0 | 0 | 0 | 0 | 0 | 0 | 1 | 1 | 1 | 1 |
| G10 | 0 | 0 | 0 | 0 | 0 | 0 | 0 | 0 | 0 | 0 | 0 | 0 | 0 | 1 | 1 | 1 | 1 | 1 |
| G9 | 0 | 0 | 0 | 0 | 0 | 0 | 0 | 0 | 0 | 0 | 0 | 0 | 1 | 1 | 1 | 1 | 1 | 1 |
| G8 | 0 | 0 | 0 | 0 | 0 | 0 | 0 | 0 | 0 | 0 | 0 | 1 | 1 | 1 | 1 | 1 | 1 | 1 |
| G7 | 0 | 0 | 0 | 0 | 0 | 0 | 0 | 0 | 0 | 0 | 1 | 1 | 1 | 1 | 1 | 1 | 1 | 1 |
| G6 | 0 | 0 | 0 | 0 | 0 | 0 | 0 | 0 | 0 | 1 | 1 | 1 | 1 | 1 | 1 | 1 | 1 | 1 |
| G5 | 0 | 0 | 0 | 0 | 0 | 0 | 0 | 0 | 1 | 1 | 1 | 1 | 1 | 1 | 1 | 1 | 1 | 1 |
| G4 | 0 | 0 | 0 | 0 | 0 | 0 | 0 | 1 | 1 | 1 | 1 | 1 | 1 | 1 | 1 | 1 | 1 | 1 |
| G3 | 0 | 0 | 0 | 0 | 0 | 0 | 1 | 1 | 1 | 1 | 1 | 1 | 1 | 1 | 1 | 1 | 1 | 1 |
| G2 | 0 | 0 | 0 | 0 | 0 | 1 | 1 | 1 | 1 | 1 | 1 | 1 | 1 | 1 | 1 | 1 | 1 | 1 |
| G1 | 0 | 0 | 0 | 1 | 1 | 1 | 1 | 1 | 1 | 1 | 1 | 1 | 1 | 1 | 1 | 1 | 1 | 1 |
| G0 | 1 | 1 | 1 | 1 | 1 | 1 | 1 | 1 | 1 | 1 | 1 | 1 | 1 | 1 | 1 | 1 | 1 | 1 |

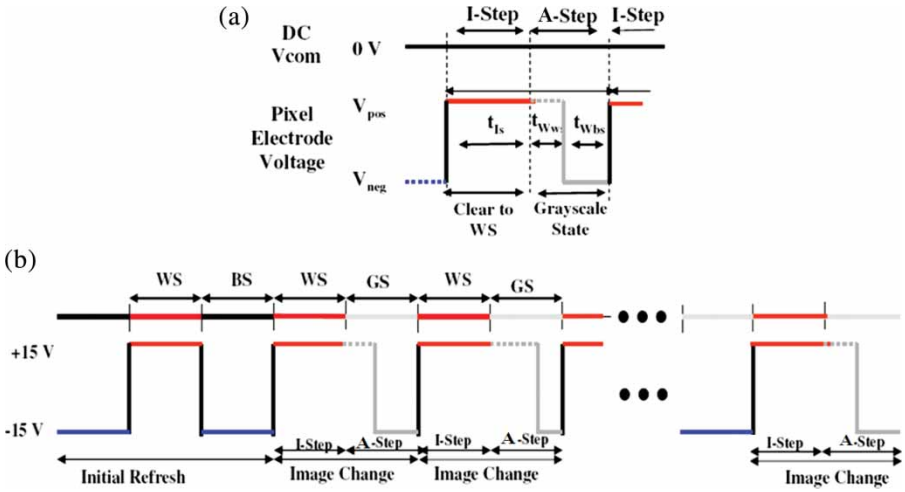


Figure 8. Modified driving method.

the lookup table is used in A-step, states 0 and 1 indicate 'idle' and $V_{neg}$ ($= -15$ V), respectively. A multiplexer (MUX) is used to select the different modes and supply voltages.

The new reduced waveform lookup table is capable of storing more driving waveforms for various temperature conditions because the electro-optical response of the EPD film is temperature-dependent and nonlinear. For different temperature conditions, the waveforms may be different. Thus, the waveforms should be able to fine-tune to the appropriate temperature. More waveforms can be stored in a smaller driving waveform lookup table.

### 3.2. *New driving method for high image quality*

The display quality and time needed to update an image can be improved by modifying the method described in Figure 5(a) [11]. Based on the gray-level definition presented in Section 3.1, the defined WS, G15, is the maximum lightness in the EPD employed, and is the actual WS. In other words, the lightness will never be increased at G15, even with the further application of a positive voltage (i.e. the image will never be whiter). On the other hand, the defined BS, G0, is not the minimum lightness. At G0, the image may be darker when negative voltages are further applied. As the defined BS is not the darkest state, a residual image appears [4].

Figure 8 illustrates the improved driving method. I-step contains only the 'clear to WS' operation and applies 40 frames of $+15$ V to make sure that the EPD will be driven to the actual WS. The driving time for achieving the actual WS of the EPD depends, however, on the characteristics of the EPD film. When an image is updated, I-step first clears to WS, and then the appropriate grayscale is applied for updating the image. Assume that the grayscale of the updated image contains $f_{Wws}$ frames with WS, and then $f_{Wbs}$ frames, where $f_{Wws} + f_{Wbs} = f_W$. As at the end of I-step, the pixel is at WS, due to the bi-stability, the first $f_{Wws}$ frames of A-step are idle, and then the remaining $f_{Wbs}$ frames are with BS, as shown in Figure 8(a). Figure 8(b) shows the detailed

driving waveforms, including the initial refresh procedure and a sequence of image updates.

## 4. Hardware design and experiment results

This section describes the hardware design of the proposed controller and presents the results of the experiment.

### 4.1. *Hardware design*

Figure 9(a) shows the block diagram of the developed display controller and its interface to the AMEPD panel. The controller consists of three major blocks: the core control unit with the attached Synchronous Dynamic Random Access Memory (SDRAM), the Serial Peripheral Interface (SPI) flash, and the power supply. The SDRAM is used as an image or frame buffer when data updating is in progress. The SPI flash stores the driving waveform files. Note that different EPD films may adopt different driving waveform files. Finally, the power supply provides the voltages to the source/gate drivers and $V_{com}$. Figure 9(b) shows the interface data signals and the power signals between the controller and the display. In this implementation, the controller is implemented by two separate boards: the controller board and the power board. The controller board is realized by the field programmable gate array (FPGA) and memory components.

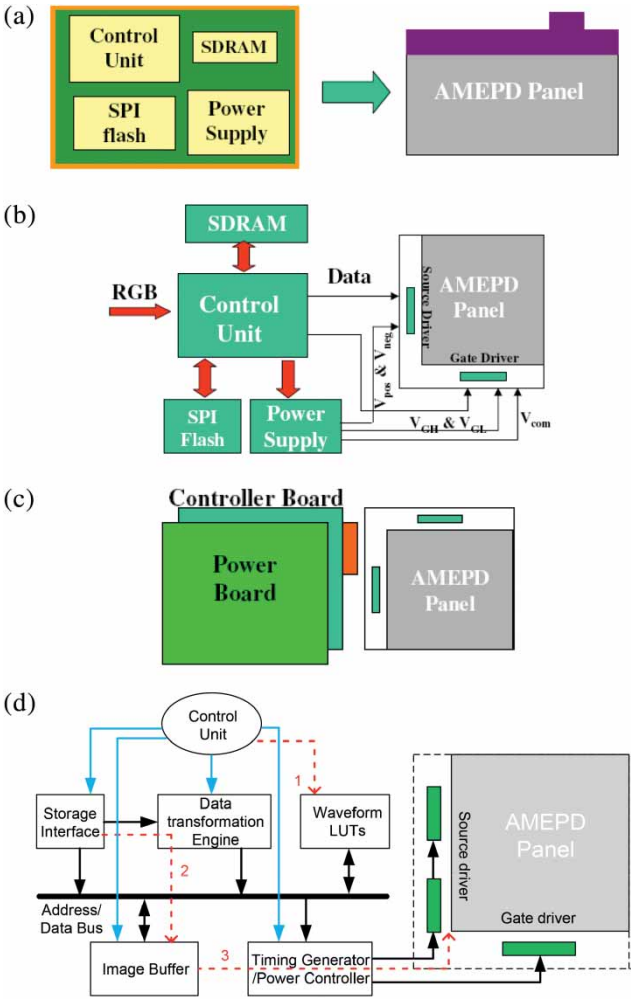


Figure 9. AMEPD controller: (a) block diagram; (b) basic operation and signal flows; (c) board-level structure; and (d) hardware architecture of the proposed controller.

As shown in Figure 9(d), three operational modes are run in the controller. First, the controller writes or edits different driving waveforms into lookup table (LUT) for the selection of various temperature conditions, because EPD films are temperature sensitive. Second, the controller reads the image from the storage device when the user presses the button for displaying a new image. The main function of the data transformation engine is to transform the RGB signals to Y presents luminance; UV presents chrominance (YUV) signals to display the AMEPD panels. Then the processed data are written into the image buffer. Third, the controller reads the data from the image buffer and generates the related timing and power-controlled signals by the timing generator and power controller. The display of a new image is completed in the three steps above.

To demonstrate the effectiveness of the proposed process for the determination of the gray levels, the 16 gray levels have been clearly shown in Figure 7(e). Figure 10 presents the prototyped display controller, which consists of two modules: the controller module and the power module. The controller module is realized by the FPGA and memory units. The board dimension is approximately (12.5 × 15.5 cm). The power module is placed on top of the controller module. The power module includes the DC/DC converter and a card reader. It takes the input power signal, 12 V, and provides various voltage levels through the output voltage control unit.

### 4.2. *Experiment results*

Based on the driving method described in Figure 5(a), at the end of I-step, the panel stays at WS. Then, at A-step, the panel is idle for the $f_{Wws}$ frames (i.e. stays at WS) and

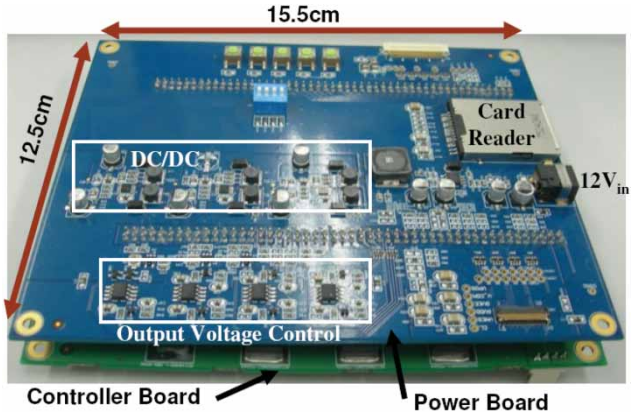


Figure 10. Display controller module.

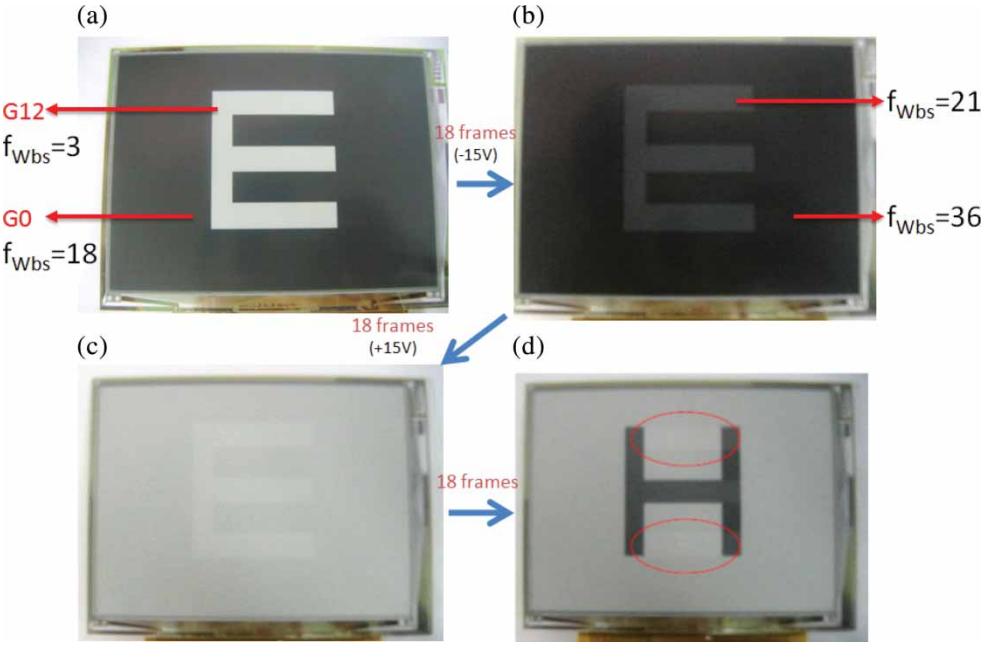


Figure 11. Residual images.

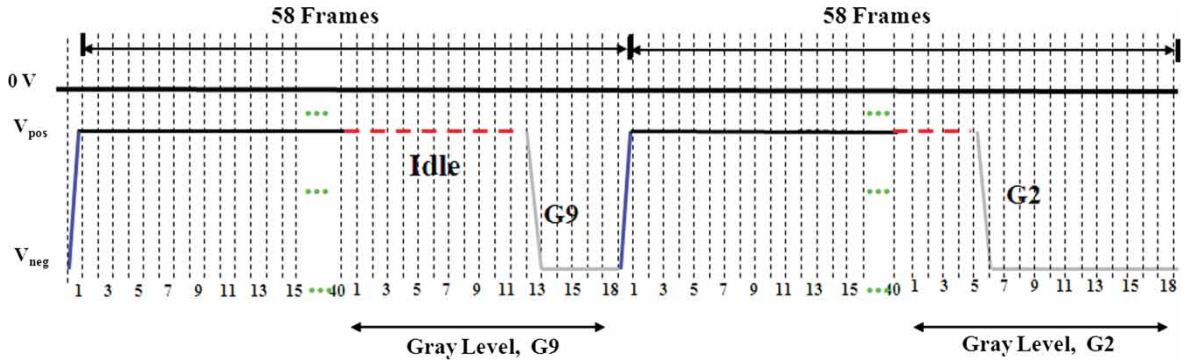


Figure 12. Modified sequence driving waveform.

then goes to the BS for the $f_{Wbs}$ frames. When the image is updated, I-step starts with 'clear to BS'. Thus, a negative voltage is applied to all the particles for the $f_{Ibs} = f_w$ frames to change to BS. As a result, a negative voltage may be applied to some particles for the $(f_{Wbs} + f_{Ibs})$ frames to change to BS.

Figure 11(a) displays the letter E with a gray level G12, where the background is black (i.e. G0). Here, $f_{Wbs} = 3$ for the pixels of letter E, and $f_{Wbs} = 18$ for the others. If a negative voltage is applied to all the pixels at 18 frames, it will result in 21 frames of negative voltages applied to the pixels of letter E, and 36 frames applied to the others, as shown in Figure 11(b).

As shown in Figure 7(b), the black background in Figure 11(a) was defined at frame 18, and it is actually not black. Continuously applying a negative voltage for more frames will make the background darker. Note that the pixels of letter E in Figure 11(b) are supposed to be darker than the background in Figure 11(a). After completing the process 'clear to BS', the step 'clear to WS' is processed. A positive voltage is applied to all the pixels. As a result, the letter and the background will not be at the same level of the WS. After I-step, the panel is supposed to stay at WS. The image of letter E, however, can still be seen in Figure 11(c). Thus, when the new image, letter H, is displayed, the residual image of letter E can still be seen in Figure 11(d).

Based on the driving method described in Figure 8(a), however, Figure 12 illustrates a sequence of voltage state transitions, where an image is updated using 58 frames. At the end of I-step, the image stays at WS. Consider a pixel with G9. Based on Table 1, $f_w = 18$, $f_{Wws} = 12$, and $f_{Wbs} = 6$. When the pixel with G9 is displayed during A-step, the first 12 frames are idle, and negative voltages are applied to the remaining six frames. Similarly, a pixel with G2 is being updated, where $f_{Wws} = 5$ and $f_{Wbs} = 13$. During I-step, the panel performs the operation of 'clear to WS'. Then, at A-step, the panel is idle for five frames and then goes to BS for the following 13 frames.

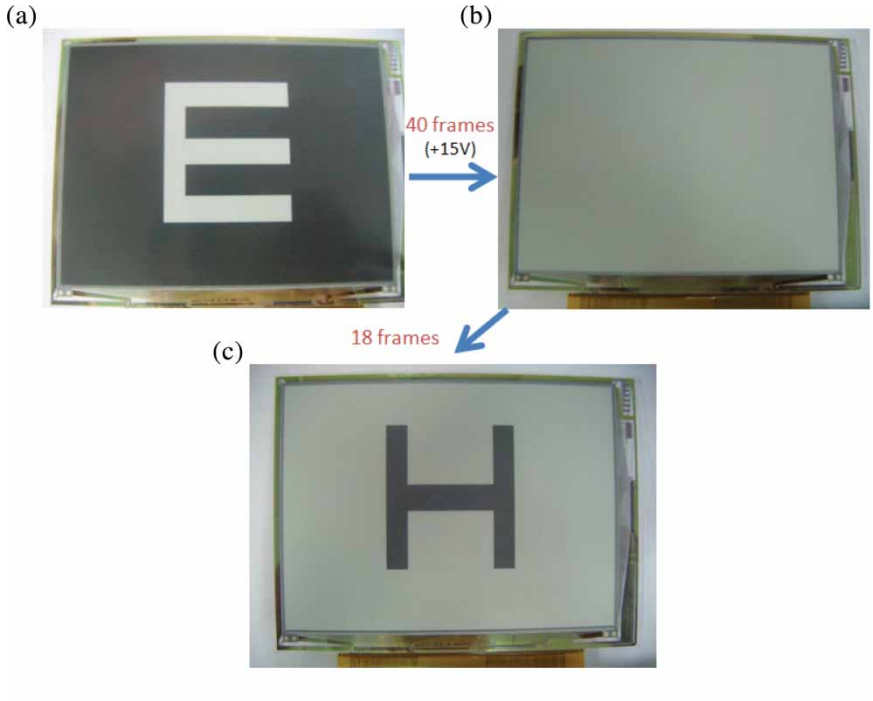


Figure 13. Displayed images.

The experiment results show that the driving method can effectively resolve the residual image problem. The patterns applying the controlled method shown in Figure 10 are repeated for the same controller with the modified driving method. Figure 13 shows the experiment results, where the residual images have disappeared.

Figure 14 shows the results of the experiment on the image display and the display quality. In this experiment, the panel displays the first image, as shown in Figure 14(a), which is that of an article in Chinese characters. The page shown in Figure 14(a) is updated by an image shown in Figure 14(b) based on the driving method in Figure 5(a). The residue of the previous image can still be visualized at the white background. On the other hand, with the modified driving method in Figure 8(a), the residue of the previous image disappears, as shown in Figure 14(c).

The modified driving method provides high-quality images and achieves high-speed performance for updating images. Note that the current commercial displays take more than 1 s to update an image. The proposed method, on the other hand, takes 58 frames, or 0.97 s, to do so.

In a previous work [11], the driving method involving clearing the previous image via initialization (I-step) and addressing (A-step), as shown in Figure 5(a), is used. Based on the measurement result shown in Figure 7, however, the WS of EPD particles was shown to be virtually invariant when 40 frames of +15 V were applied to drive the EPD to the WS from frames 0 to 40. It is important to avoid producing the residual images of the previous image when displaying a new image. Therefore, in this paper, a new driving method for high image quality is proposed, as shown in Figure 8(a). In the related experiments shown in Figures 11 and 13, a good image quality was obtained, and the issue of residual images was avoided, when the new driving method was used. Table 2 shows the advantages of the proposed lookup table and driving method.

### 4.3. *Further quality improvement*

Figure 15 shows the results of the experiment on the display of an article on a 6" AMEPD panel connected to the controller in Figure 10. The image quality is reasonably good.

The experiments that were conducted in this study were based on the existing EPD, which cannot be modified by the users. A number of suggestions to EPD producers, however, are discussed herein for further quality improvement of handheld reading devices.

First, the source driver of the existing AMPED generally receives 4 pixels (D[0:1], D[2:3], D[4:5], and D[6:7]) at each clock cycle, where each pixel contains two bits. For the 6" EPD with an 800 × 600 resolution, it takes 200 cycles to complete the display of one line (800 pixels). With the same source driver structure, the proposed method requires an only-1-bit format and will take only 100 cycles to complete the same display. Thus, the source driver can be modified using one bit for each pixel to reduce the pin count, or can take 8 pixels at a time to speed up the display performance.

As the driving methods described in Figures 5(a) and 8(a), 'clear to WS' and 'clear to BS' are achieved by the patterns G15 and G0 in Table 1, respectively. It is possible to define a mode in the source IC of the AMEPD for these two

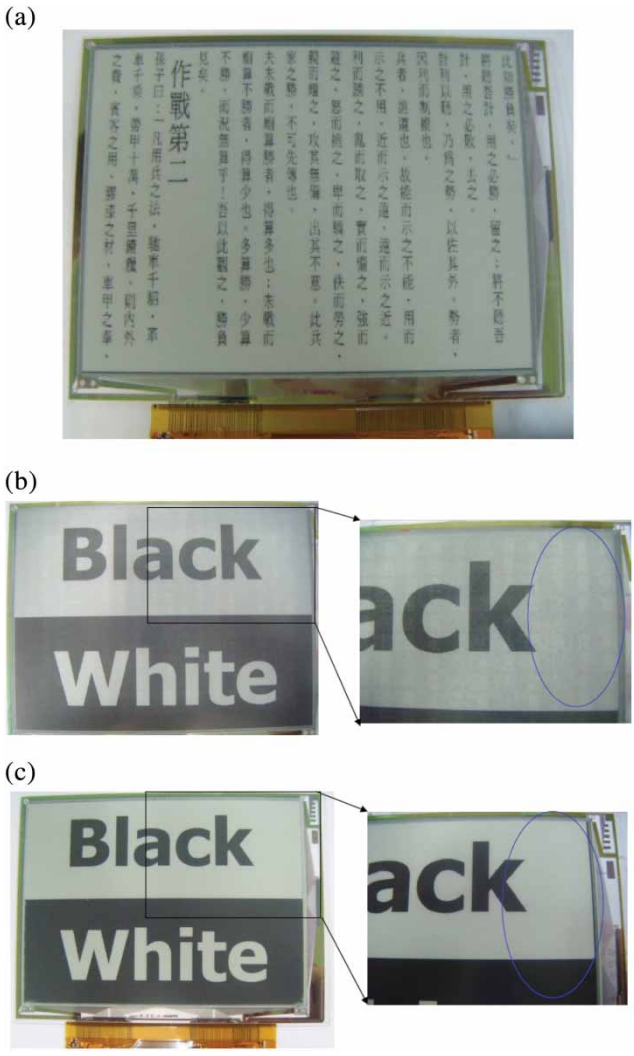


Figure 14. Experiment results.

Table 2. Advantages of the proposed lookup table and driving method.

| | Traditional lookup table | Proposed lookup table |
|---|---|---|
| Memory size | $2^*n^*n^*f_w$ | $n^*f_w$ |
| Residual images | Traditional driving method Produced | Proposed driving method Eliminated |

operations and the required number of frames. Thus, it is not necessary to transmit such patterns to reduce the power consumption for handheld reading devices. At this moment, where the existing source IC of the AMEPD supports 25 MHz in dot clock (DCLK), the data transmission with the frame rate of 60 Hz is not on the critical path. Thus, the data transmission is still workable at the cost of greater power consumption. When the frame rate is more than 100 Hz, however, and the resolution is more than 800 × 600, the data transmission time may be longer than what DCLK can handle. As such, the suggested modification becomes important and necessary for quality improvement.


Figure 15. 6” AMEPD panel with a microcapsule structure.

## 5. Conclusions

For the e-book and e-newspaper applications, this paper presents the implementation of the high-performance display controller for microcapsule AMEPD panels. This study proposed a new reduced waveform lookup table to reduce the lookup table size and to speed up the display time. The smaller the table size is, the greater the number of waveforms that can be stored in the same amount of memory space. As a result, the waveforms for various temperature conditions can be readily downloaded to enhance the functionality. The straightforward approach for the determination of the gray levels provides the salient function of quickly fine-tuning the waveforms while still providing an acceptable gray-level quality. The prototyped controller was connected to a 6” AMEPD panel, whose excellent display quality demonstrated the effectiveness of the proposed controller design.

The proposed design takes 58 frames, or 0.97 s, to update an image. The performance is reasonably good for smart handheld reading devices. The updating performance can be further improved, however, if the scanning frame rate of the AMEPD will be increased.

## Acknowledgements

The authors are grateful to the anonymous referees for providing many valuable comments that has improved the quality of this paper. The authors thank H.-H. Chen, J.-S. Liao, M.-C. Weng, Y.-C. Su, D.-W. Kuo, K.-C. Chiu, Y.-C. Chen, W.-T. Tseng, C.-R. Lee, and H.-T. Yu at CPT Inc. for co-developing the AMEPD system with them.

## References

[1] A. Henzen, J. van de Kamer, T. Nakamura, T. Tsuji, M. Yasui and M. Pitt, *SID Symposium Digest* (Development of Active Matrix Electronic Ink Displays for Handheld Devices, America, 2003), pp. 176–179.

[2] R.C. Liang, J. Hou, H. Zang and J. Chung, *Passive Matrix Microcup Electrophoretic Displays* (IDMC, Taipei, 2003).

[3] A. Henzen and J. van de Kamer, *IMID Digest* (Perspectives and Challenges of Electrophoretic Displays, Korea, 2005), pp. 236–240.
[4] A. Henzen and J. van de Kamer, *SID Symposium Digest* (High Quality Images on Electronic Paper Displays, America, 2005), pp. 1666–1669.
[5] I. Ota, J. Ohnishi and M. Yoshiyama, Proc. IEEE **61** (7), 832–836 (1973).
[6] B. Fitzhenry-Ritz, IEEE Trans. Electron Devices **28** (6), 726–735 (1981).
[7] R.C. Liang, J. Hou, H. Zang, J. Chung and S. Tseng, J. SID **11** (4), 621–628 (2003).
[8] A. Henzen, J. Kamer, T. Nakamura, T. Tsuji, M. Yasui, M. Pitt, G. Duthaler, K. Amundson, H. Gates and R. Zehner, J. SID **12** (1), 17–22 (2004).
[9] M.T. Johnson, G. Zhou, R. Zehner, K. Amundson, A. Henzen and J. Kamer, J. SID **14** (2), 175–180 (2006).
[10] K. Amundson and T. Sjodin, *SID Symposium Digest* (Achieving Graytone Images in a Microencapsulated Electrophoretic Display, America, 2006), pp. 1918–1921.
[11] C.-M. Lu and C.L. Wey, IEEE J. Display Technol. **7** (8), 434–442 (2011).